Published in the Proceedings of the 16th International Aluminum Alloys Conference (ICAA16) 2018
ISBN: 978-1-926872-41-4
by the Canadian Institute of Mining, Metallurgy & Petroleum

SIMULATION OF EXTRUSION PROCESSES OF ALUMINUM PROFILES WITH MODELING OF MICROSTRUCTURE

*D.-Z. Sun, A. Ockewitz, A. Trondl

Fraunhofer Institute for Mechanics of Materials IWM
Woehlerstrasse 11, 79108 Freiburg, Germany
*(*Corresponding author: dong-zhi.sun@iwm.fraunhofer.de)*

ABSTRACT

Numerical simulation of extrusion processes offers an efficient method for tool design and optimization of geometries and properties of extruded parts. However, until now there are few systematic investigations about influences of material model and different parameters e.g. for friction and thermal processes on calculated local and global responses. Since extrusion processes are essentially influenced by friction between billet and extrusion tools, new friction tests were performed in this work to develop a reliable friction model. Compression and torsion tests were performed at different temperatures and velocities to calibrate the material model for extrusion simulations. Extrusion processes for circular rods and U-profiles were conducted at TU Berlin with backward and forward extrusion for different extrusion ratios, billet temperatures, product velocities and cooling conditions. This work focuses on numerical simulations of the extrusion tests with the FE code HyperXtrude. Based on the calculated distributions of local strain, strain rate and temperature the recrystallized volume fraction and grain sizes were calculated with empirical models and compared with the experimental results from optical micrographs and EBSD scans. The calculated total and friction forces and temperatures were compared with the experimental results and the deviations between experiment and simulation were analyzed.

KEYWORDS

Aluminum profiles, Extrusion simulation, Friction test, Modeling of microstructure, Torsion test

INTRODUCTION

Extruded aluminum components are widely used in vehicle constructions due to light weight and manufacturing consideration. Local mechanical properties in the components are inhomogeneous as a consequence of the spatial distribution of microstructure which is influenced by numerous factors like material composition, temperature, tool design, friction, extrusion ratio and speed during the extrusion process. For the optimization of the extrusion process with regard to all these factors numerical simulation can be an essential tool. Based on results of finite element simulations of the extrusion process the microstructure in the extruded components can be predicted and then the resulting mechanical properties can be numerically determined instead of by costly trial and error methods. The aim of the work presented in this paper is the development of a numerical method for the simulation of extrusion processes with modeling of microstructure.

The basis for a reliable extrusion simulation is the selection and calibration of a temperature and strain-rate dependent material model, a friction model and models for calculation of microstructure. One difficulty for the determination of stress vs. strain curves for an extrusion simulation is that local strains in an extrusion process of aluminum profiles can reach very high values e.g. about 30 (Mehtedi, 2015) and the standard hot compression tests can only deliver experimental data to a maximal strain less than 1. The hot torsion test is capable of producing strains of the order of 100 without the instabilities, which are caused by barreling and necking in compression and tension, respectively (Mehtedi, 2015). Since the stresses and strains over the cross section of torsion specimens are inhomogeneous and the evaluation method is complex due to the large plastic deformation, the results from the torsion tests have to be verified.

Extrusion processes, especially direct extrusion, are remarkably influenced by friction between billet and extrusion tools. The friction force at the beginning of a direct extrusion amounts to a large part of the total extrusion force and strongly decreases during the extrusion process due to the reduction of contact area. The microstructure and mechanical properties of extrudates depend considerably on friction effects (Ockewitz, 2012). One severe problem with friction is that larger local strains and strain rates and higher temperatures at contact areas lead to the formation of coarse grain zones at the surfaces of an extruded aluminum profile. Inhomogeneous microstructure over a cross section especially with coarse grain zones is not desirable. A reliable determination of friction behavior is important for the construction of extrusion tools and optimization of whole extrusion processes. Common friction tests like pin-on-disk do not give relevant information about friction in extrusion situations due to lower hydrostatic stresses. There are few results about influence of normal stress, temperature and velocity on friction (Karadogan, 2010, Hora, 2012). Due to the lack of reliable experimental results about friction behavior during an extrusion process, friction is usually considered as sticking in numerical simulations. In this work a new friction test setup is suggested and simulated. Since the friction test is nearly a small scale extrusion test, the real loading conditions during extrusion processes like high hydrostatic stress and large plastic deformation can be achieved.

During the thermo-mechanical processes in hot extrusion different recrystallization mechanisms like static or dynamic recrystallization or grain growth can take place. Empirical and physical models for the description of these mechanisms have already been developed and verified by experimental and numerical investigations (Sheppard, 2003, Schikorra, 2008). A problem is that the contribution of each mechanism to the final microstructure cannot be easily determined. The occurrence of static recrystallization can however be suppressed by cooling the extrudate immediately after deformation. By comparison of the microstructure in extrudates with and without additional cooling at least the effects of static and dynamic recrystallization can be distinguished. The extrusion tests performed in this work for the validation of simulation results were designed to produce static as well as dynamic recrystallization and varying local distributions of strain, strain rate and temperature in the extruded parts.

TORSION TESTS AND SIMULATIONS

Torsion specimens from EN AW-6005A were tested at three temperatures (400°C, 450°C and 500°C) and four rotation velocities (1.8°/s, 18°/s, 180°/s and 720°/s). The torsion specimens have a total length of 150 mm. The diameter and length of the testing region are 12 mm and 8 mm, respectively. Before a test the axial load was set to zero and the axial position of the torsion specimen was fixed during the test. The torque, number of revolutions and temperatures at three positions were measured during the test. Figure 1 shows the torsion specimen and compares the testing section before and after test at 450°C. Obviously the large plastic deformation of the region with the smallest diameter results in the formation of a pronounced rough surface. Metallographic investigation shows clearly that the surface has a wave contour due to inhomogeneous yielding. Moreover, several voids and micro cracks can be found at grain boundaries.

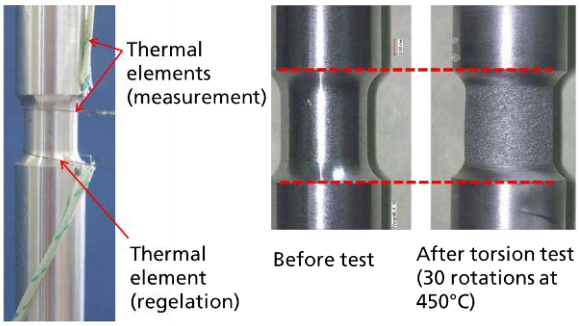

Figure 1. Torsion specimen with three thermal elements (left) and comparison of the section for testing before and after test (middle and right)

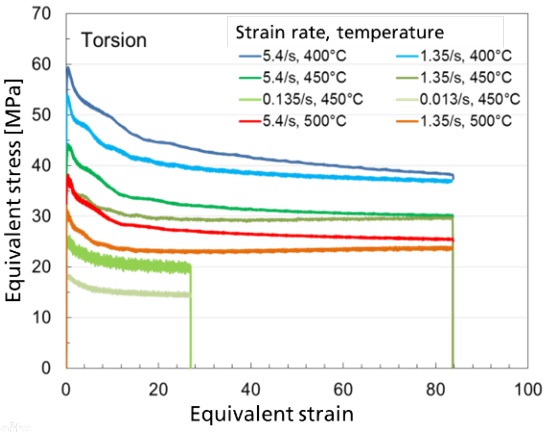

Figure 2. Equivalent stress vs. equivalent strain curves of torsion tests at three temperatures and different strain rates

To describe the deformation behavior of aluminum alloys under shear loading the von Mises equivalent stress σ and the equivalent strain ε on the specimen surface were calculated from the measured torque M and the number of revolutions N using the following equations (Dieter, 1986, Mehtedi et. Al., 2015:

$$\sigma = \frac{\sqrt{3}(3M + \theta \frac{dM}{d\theta})}{2\pi r^3} \quad (1)$$

$$\varepsilon = \frac{2\pi N r}{\sqrt{3} l} \quad (2)$$

r: radius of testing region
l: length of testing region
θ: rotation angle (2πN)
N: number of revolutions

σ: equivalent stress
ε: equivalent strain
M: torque

The above equation for the calculation of equivalent stress was derived by taking into account large plastic deformation. In this case the shear stress has not a linear relationship with the radius and the maximum shear stress on the surface is no longer proportional to the torque. Since the contribution of the second term in Equation 1 to the total value is very small, it was not taken into account at the calculation of the equivalent stress in this work. Figure 2 compares the equivalent stress vs. equivalent strain curves from the torsion tests for different testing temperatures and strain rates. It can be recognized that the flow stress increases considerably with increasing strain rate and decreasing temperature. The torsion tests deliver stress vs. strain curves up to a strain of 85 without rupture. The flow stress reaches a maximum value at a strain about 0.6, after that it reduces to a stabilized level with increasing deformation. Figure 3 compares the stress vs. strain curves from the hot torsion tests with the results from hot compression tests (Ockewitz,

2012) for test temperature 450°C and three strain rates. The results of the both specimen types agree up to a strain of 0.6, then the flow stresses from hot compression tests deviate from the values of torsion tests due to a remarkable rising with deformation, which may be attributed to the barreling process in the compression specimens.

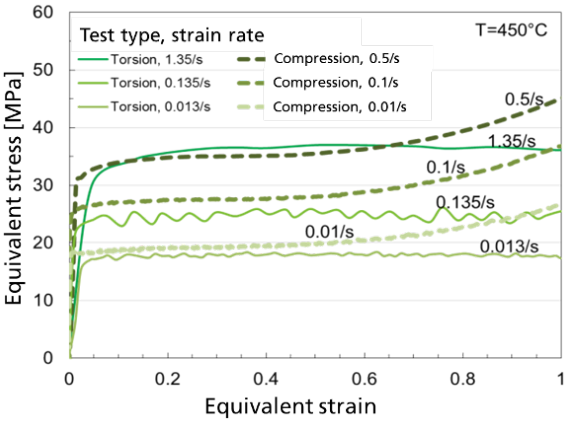

Figure 3. Comparison of the equivalent stress vs. equivalent strain curves from torsion and compression tests at 450°C and different strain rates

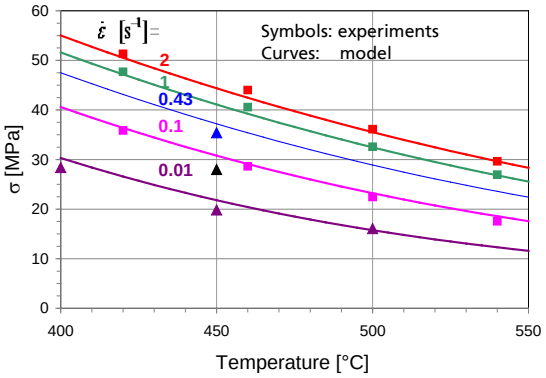

Figure 4. Measured temperature and strain rate dependence of the flow stress at a strain of 50 percent from hot compression tests, in comparison with the results calculated with the Zener-Hollomon model

Material models in different FE programs for extrusion simulations, e.g. HyperXtrude and DEFORM, are based on the Zener-Hollomon parameter Z:

$$\sigma = \frac{1}{\alpha} Sinh^{-1}\left(\left[\frac{Z}{A}\right]^{1/n}\right), \qquad (3)$$

$$Z = \dot{\varepsilon}\exp(\Delta H / RT)$$

ΔH = 177500 J/mol
n = 5
A = 7.55454E+10 s^{-1}
α = 3.96E-08 Pa^{-1}

The results of the hot compression tests were used to fit the corresponding parameters of the material model. The determined model parameters are given beside Equation 3. Figure 4 shows the good agreement between the measured flow stresses at a strain of 50% and the calculated curves from the Zener-Hollomon model for different temperatures and strain rates.

Torsion tests were simulated with different formulations in the FE code ABAQUS. Both the ALE (Arbitrary Langrangian Eulerian) formulation and the pure Eulerian formulation were used to treat the extremly large plastic deformation in the torsion specimens. The third simulation technique using 2D axisymmetric elements with twist in ABAQUS/Standard delivers the most efficient solution. These elements have a degree of freedom for rotation angle besides axial and radial displacements. The stress vs. strain curves used for the simulations were obtained from the calibrated Zener-Hollomon model. Experimental results show that the temperature in the torsion specimens increases due to the transformation of plastic work into heat. Therefore, the simulations were performed with thermal mechanical coupling or the assumption of adiabatic heating (without heat conduction). Figure 5 shows the calculated equivalent plastic strain on the undeformed mesh (a) and the calculated von Mises equivalent stress on the deformed mesh (b). Both plots in Figure 5 were obtained after three revolutions. Figure 6 compares the measured and calculated torque vs. number of rotations curves for three rotation velocities at 450°C. The maximum values of torque were well predicted. While the maximum value of the torque is hardly affected by the assumed condition for thermal conduction, the slope of the torsion moment vs. number of rotations curves depends strongly on it. The application of thermal mechanical coupling is not enough to obtain the

measured reduction of torsion moment with increasing deformation. The good agreement between experiment and simulation shown in Figure 6 is achieved using the adiabatic condition (without heat conduction), which is not true especially at low rotation velocities. The intensified softening effect caused by using the adiabatic condition in the simulations compensates just the damage effect in the real specimens.

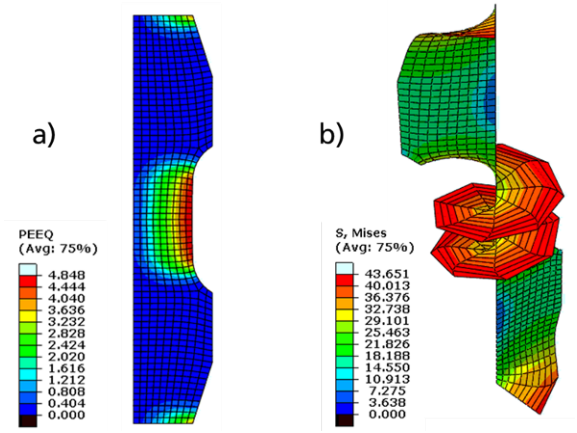

Figure 5. a) Calculated plastic equivalent strain on undeformed mesh, b) calculated von Mises equivalent stress on deformed mesh after three revolutions at 450°C and velocity 180°/s

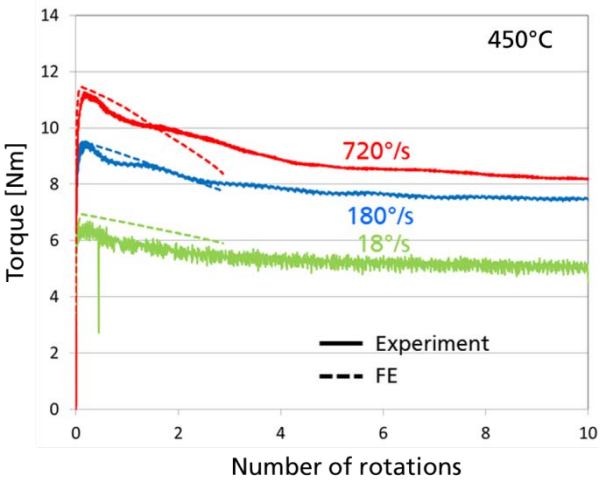

Figure 6. Torque vs. number of rotations measured at 450°C and three rotation velocities in comparison with the results calculated with ABAQUS

FRICTION TESTS AND SIMULATIONS

To enable large plastic deformation of the specimen during a friction test under high hydrostatic loading a new test setup was suggested which is depicted in Figure 7a. In this test a ring-shaped aluminum specimen is placed between a steel mandrel and a ring-shaped steel die with open bottom. The specimen is pressed by a hollow steel punch from top to bottom like in forward extrusion. During the test the punch displacement is recorded and forces are measured at the punch and the mandrel. The friction tests were conducted at 420°C, 460°C and 500°C with punch velocities of 0.1 and 0.2 mm/min. Two die geometries with conical and cylindrical bottom were used (Figure 7b).

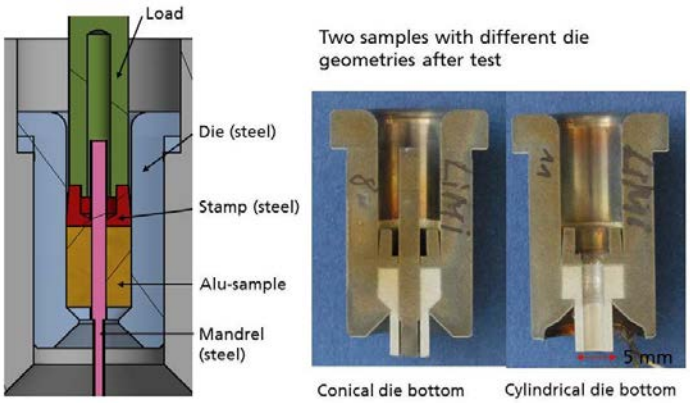

Figure 7. a) first setup of the high pressure friction test with large plastic deformation, b) two cuts of samples with two different die geometries after friction test

After the first friction tests the setup was optimized by increasing the outer and inner diameters of the samples to avoid buckling of the mandrel and to increase the extrusion ratio. Only the die with cylindrical bottom was applied for further investigation since the die with conical bottom did not show any advantage. The outer and inner diameters of the optimized samples are 16 mm and 5 mm, respectively. The outer diameter of the samples was reduced to 7 mm after the friction test and the inner diameter remains at 5 mm. Figure 8a shows the cross section of a sample after friction test at 420 °C, 0.2 mm/min with the cylindrical die. Flow lines in the specimen and a dead zone above the die can be clearly recognized. Figure 8b and c show grain distribution measured with EBSD method in the sample. The grain boundaries were defined based on orientation differences more than 2°, 5° and 15°. The grains at contact surfaces between die and sample and between mandrel and sample are smaller than in the center of the sample.

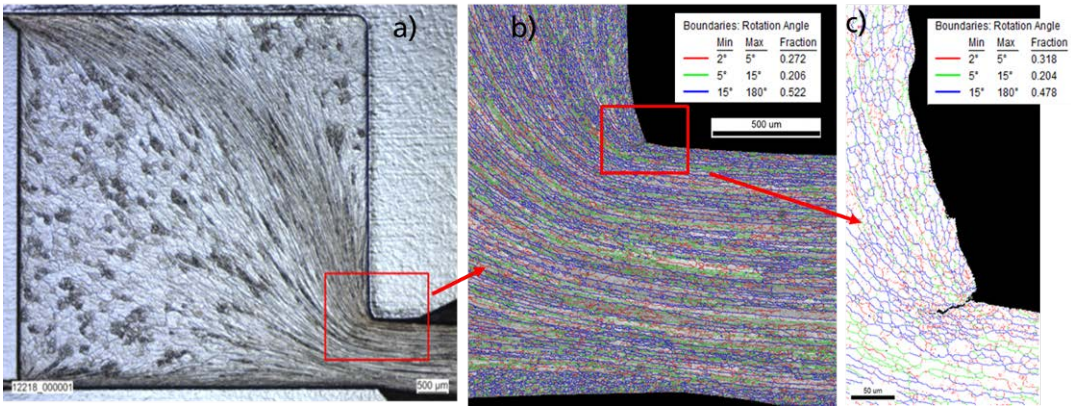

Figure 8. Cross section with grain distribution measured with EBSD after friction test at 420 °C, 0.2 mm/min with the cylindrical die

The measured punch force and friction force between the sample and the mandrel are shown in Figure 9 and Figure 10 as function of punch displacement for three testing temperatures and three testing velocities, respectively. The friction force was measured at the mandrel. The initial velocity of two friction tests at 420°C was increased after a punch displacement of about 3 mm. Both testing temperature and velocity have a large influence on the measured punch and friction force. A higher testing velocity or a lower temperature leads to a significant rise of the punch force and the friction force.

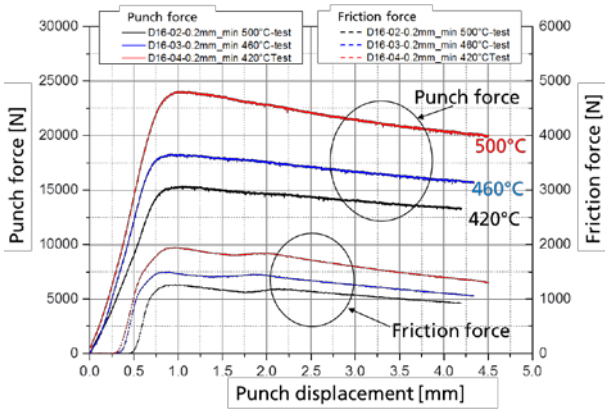

Figure 9. Measured punch force and friction force as function of punch displacement for three testing temperatures at 0.2 mm/min

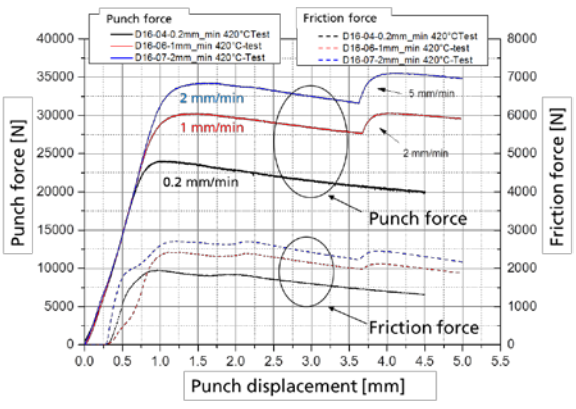

Figure 10. Measured punch force and friction force as function of punch displacement for three testing velocities at 420°C

The friction tests were simulated with HyperXtrude and ABAQUS/Explicit. While HyperXtrude cannot model the filling process, ABAQUS/Explicit is able to model the whole deformation process of the friction test. To reduce the simulation expense one segment with 15° of the sample was modelled with ABAQUS/Explicit using the corresponding boundary conditions. The sample was modeled with Eulerian formulation and the die, punch and mandrel were modeled with Langrangian formulation to achieve an efficient and precise solution. As in the simulation of torsion tests the temperature and strain-rate dependence of the flow behavior measured with the hot compression tests was used in the simulations of friction tests. The contacts between the sample and tools were modelled using the Coulomb friction model with a friction coefficient which increases from 0.14 to 0.24 with increasing sliding velocity from 0 to 10 mm/s.

Figure 11 shows the finite element model for the friction test and the calculated distributions of equivalent plastic strains at three different punch displacements. Large plastic deformation at the bearing and the influence of the contact surfaces on the strain distribution can be recognized. Figure 12 compares the measured and calculated cross section of a sample after the friction test. Obviously the flow lines, the dead zone and the gaps between the tools and the sample observed at experiment can be well predicted by the numerical simulation.

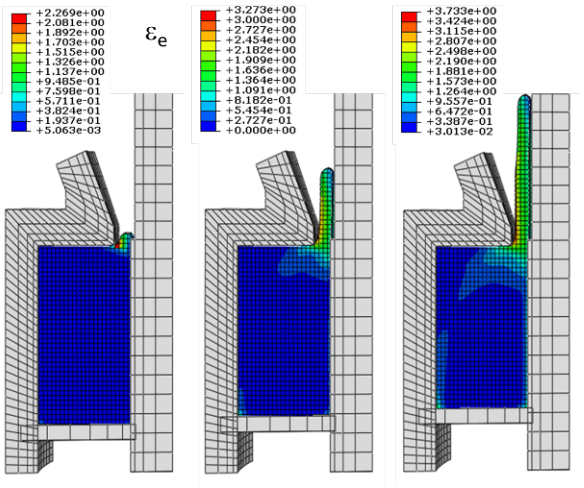

Figure 11. Simulated deformation of a sample in a friction test at three punch displacements with the distribution of equivalent plastic strain

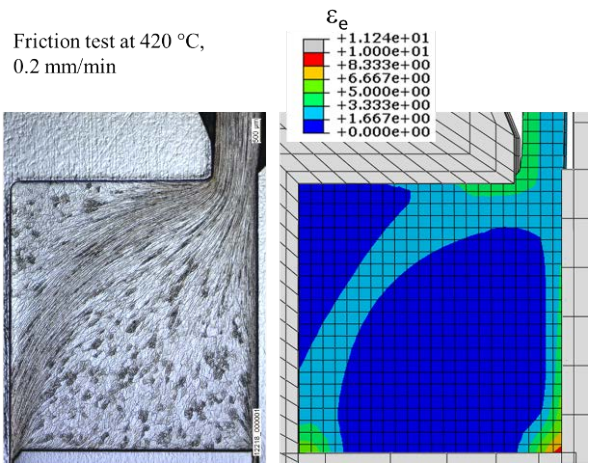

Figure 12. Cross section of a sample after friction test (left) and simulated deformation with distribution of equivalent strain (right)

Figure 13 compares the measured and calculated punch force and friction force vs. displacement curves for three friction tests at two different temperatures and two different punch velocities. Both the punch forces and friction forces for different test conditions were well predicted with the applied friction model. The measured jumps of punch and friction forces caused by changing the punch velocity from 2 mm/s to 5 mm/s were also reproduced by the simulation.

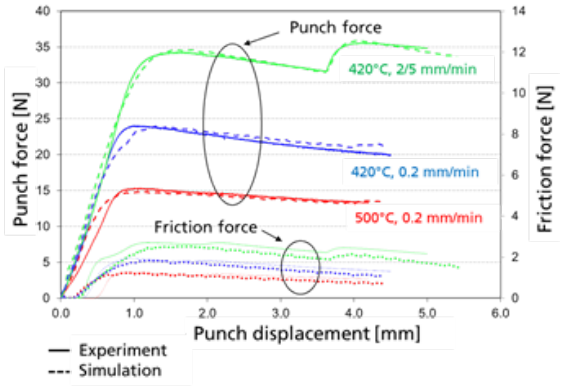

Figure 13. Comparison of measured punch force and friction force vs. displacement curves with the calculated results for different temperatures and punch velocities

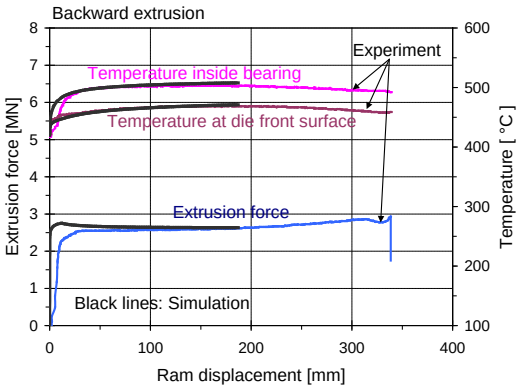

Figure 14. Measured and calculated forces and temperatures for extrusion ratio 30:1 at 460 ºC, product velocity 8 m/min (backward extrusion)

EXTRUSION TESTS AND MICROSTRUCTURE MODELING

Extrusion of Circular Rods

For the analysis of the microstructure of AA6005A and the verification of simulation results circular rods were extruded at FZS Berlin by backward as well as forward extrusion for two extrusion ratios (30:1 and 60:1), billet temperatures of 420, 460 and 500 ºC and different product velocities. The product velocities for the smaller extrusion ratio were 2, 8 and 15 m/min and for the larger ratio 4, 8, 15 and 30 m/min. The billet diameter was 125 mm, thus the rod diameter for extrusion ratio 30:1 is 23 mm and for 60:1 16 mm. In one series of tests the rods were water-cooled immediately behind the die exit, in order to prevent the possible occurrence of static recrystallization. Recrystallization observed in these rods should be attributed to dynamic recrystallization processes. In a second series of tests the rods cooled down at air.

The extrusion tests were simulated with the FE code HyperXtrude. A 3D model with quarter symmetry was used for the simulations. The die, container and punch were modeled as rigid bodies. The sine hyperbolic inverse model was used for the simulations with the parameters determined from the results of hot compression tests as described above. Friction was assumed as sticking. The heat transfer coefficient between billet and tools was set as 7000 $Wm^{-2}K^{-1}$. For the backward extrusion tests the influences of extrusion ratio, billet temperature and product velocity on punch force and temperature were calculated in good agreement with the measurements, as shown for one example in Figure 14. In the simulations of the forward extrusion tests with the same model parameters the calculated forces and temperatures are too high compared with the measurements (Figure 15). This can be attributed to the fact that the additional friction between billet and container in forward extrusion is overestimated by the assumption of sticking friction.

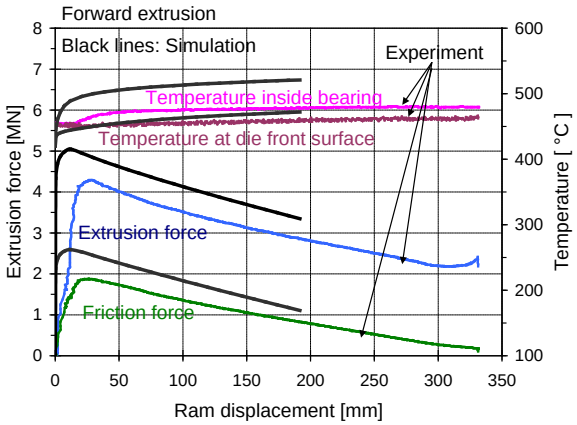

Figure 15. Measured and calculated forces and temperatures for extrusion ratio 30:1 at 460 ºC, product velocity 8 m/min (forward extrusion)

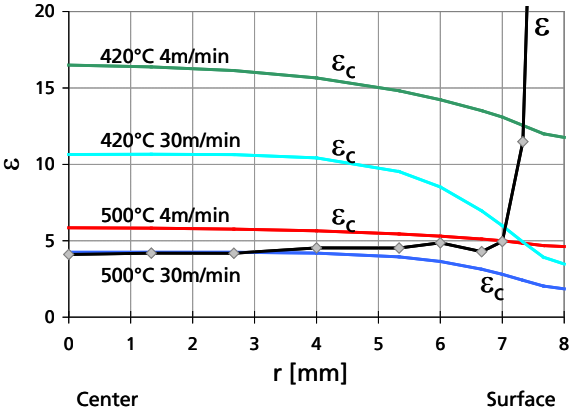

Figure 16. Radial distribution of strain ε and critical strain ε_c for activation of drx for selected backward extrusion tests, extrusion ratio 60:1

Modeling of Microstructure

As a first step in the modeling of microstructure evolution the dynamic recrystallization (drx) model from (Schikorra et.al., 2008, DEFORM, 2009) was chosen. According to this model dynamic recrystallization occurs when the strain exceeds a critical strain ε_c:

$$\varepsilon_c = a_1 \, d_0^{n_1} \, \dot{\varepsilon}^{m_1} \exp\left(Q_1 / RT\right) + c_1 . \qquad (4)$$

An Avrami equation is used to describe the relationship between the recrystallized volume fraction and the effective strain:

$$X_{drx} = 1 - \exp\left(-\beta_d \left(\frac{\varepsilon - a_{10}\varepsilon_c}{\varepsilon_{0.5}} \right)^{k_d} \right) \qquad (5)$$

where $\varepsilon_{0.5}$ is the strain for 50% recrystallization:

$$\varepsilon_{0.5} = a_5 \, d_0^{n_5} \, \dot{\varepsilon}^{m5} \exp\left(Q_5 / RT\right) + c_5 . \qquad (6)$$

The grain size is expressed as:

$$d_{drx} = a_8 \, d_0^{h_8} \, \varepsilon^{n_8} \, \dot{\varepsilon}^{m_8} \exp\left(Q_8 / RT\right) + c_8 . \qquad (7)$$

In the above equations d_0 is the initial grain size, ε the strain, $\dot{\varepsilon}$ the strain rate and T the temperature. R is the universal gas constant. All other unknown variables in Eqs. 4 - 7 are material parameters which have to be fitted to experimental results.

The parameters were determined for selected backward extrusion tests from the water-cooled test series with extrusion ratio 60:1. The distributions of temperatures, strain rates and strains through the cross-sections of the rods from the simulations were related to the microstructure of corresponding extrusion tests through Eqs. 4 - 7. For ε_c (Eq. 4) the following parameters were obtained: $a_1 d_0^{n1}$ = 2.66E-05, m_1 = -6.25E-03, Q_1 = 83320 Jmol^{-1} and c_1 = 0. Figure 16 shows the radial distribution of the computed strain ε, which is independent of temperature and velocity (black line), and of the critical strain ε_c for four selected tests. Dynamic recrystallization is activated where $\varepsilon > \varepsilon_c$. The strain for 50% recrystallization $\varepsilon_{0.5}$ in Eq. 6 was set to a constant value of 0.15 as in (Schikorra et.al., 2008). For the recrystallized volume fraction (Eq. 5) the remaining parameters are: $ß_d = k_d = a_{10} = 1$. The parameters determined for the grain size (Eq. 7) are: $a_8 d_0^{h8}$ = 4.050E+06, n_8 = 0, m_8 = -0.35, Q_8 = -65240 Jmol^{-1} and c_8 = 0. The model was implemented as a user function in HyperXtrude. The influences of product velocity and billet temperature on dynamic recrystallization can be well predicted with the determined model parameters. The calculated recrystallized

volume fraction and grain size agree as well with the experimental results for both backward extrusion (Figure 17) and forward extrusion (Figure 18). As also static recrystallization (srx) was observed in the extruded rods with air-cooling, an empirical model based on an Avrami equation for the description of this mechanism from (Sheppard, Duan, 2003) was used to simulate the corresponding extrusion tests. The computed microstructure is in good agreement with the experimental results (Ockewitz et. al., 2012).

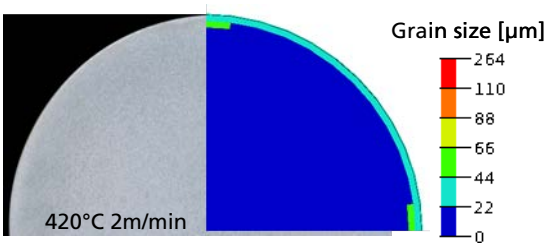

Figure 17. Calculated distributions of grain size due to drx through the cross-section for a selected backward extrusion test, ratio 30:1

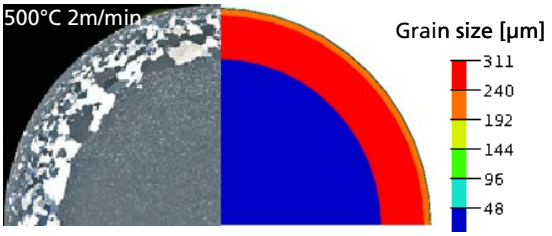

Figure 18. Calculated distributions of grain size due to drx through the cross-section for a selected forward extrusion test, ratio 30:1

Extrusion of U-Profiles

To validate the applied numerical methods U-profiles with different wall thicknesses were extruded at FZS Berlin using backward and forward processes at different temperatures, velocities and cooling conditions (Sun, Mueller, 2017). The grain sizes and recrystallized volume fractions were determined with metallography and EBSD analysis. The extrusion processes of the U-profiles were simulated with HyperXtrude and ABAQUS/Explicit based on the model parameters determined before. One half of the U-profile was modelled by using the corresponding symmetry boundary conditions. Figure 19 compares the results from experiment and simulation for a forward extrusion of a U-profile at temperature of 500°C and punch velocity of 1.1 mm/s with immediate water cooling after the extrusion. Although the measured temperatures at three positions in the bearing, the total force, the friction force and the forces on die were overestimated to different extents, the forms of the measured curves agree with the calculated ones very well. The deviations may be attributed to the assumed thermal conditions and possible deviations in geometries of the extrusion tools in experiment and simulation. Simulations of other forward extrusion tests at different process conditions show a similar agreement. The influences of temperature and press velocity on press forces and temperature changes could be predicted in a satisfactory manner. The measured force vs. displacement curves in the backward extrusion tests on the U-profiles were slightly more overestimated. This may be caused by an inaccuracy in the modeling of the complex boundary conditions in the two pockets between billet and bearing. Figure 19 also shows the calculated distribution of local strain in the U-profile during extrusion. The maximum value of local strain reaches about 21.

Metallographic investigation shows that the parameters of extrusion processes, the cooling condition and the wall thickness have a significant influence on formation of microstructure. In many cases a reduction of temperature results in the suppression of recrystallization and an increase of press velocity supports recrystallization. Figure 20 shows that narrow zones with coarse grains were formed at the surfaces of a forward extruded U-profile and the simulation could predict this effect.

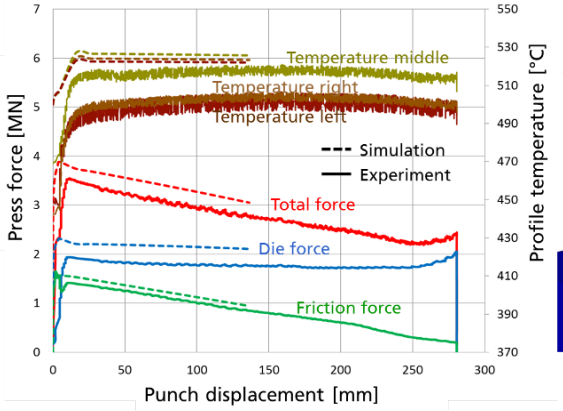

Figure 19. Measured total force, die force and friction force as function of the punch displacement for forward extrusion of a U-profile at 500°C, 1.1 mm/s, water cooling in comparison with the results calculated with HyperXtrude (left) calculated distribution of equivalent strain (right)

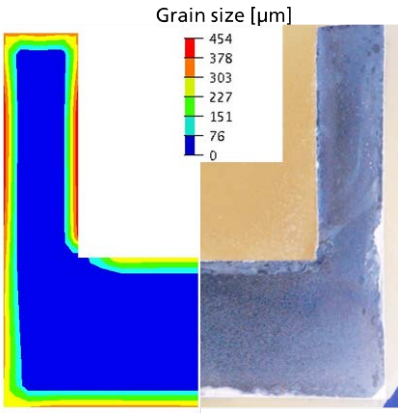

Figure 20. Calculated distributions of grain size due to drx through the half cross-section of U-profile (left) and the experimal part at 500°C, 1.1 mm/s, water cooling (right)

CONCLUSIONS

To calibrate the material and friction models for extrusion simulations hot torsion and friction tests on EN AW-6005A were performed at different temperatures and deformation velocities. As an advantage torsion tests can deliver true stress vs. strain curves up to very large strains which occur in an real extrusion process. There is no problem with instability or friction effects which take place in standard compression tests. The disadvantage of the torsion tests lies in that the performance of the torsion tests e.g concerning temperature measurement is complex and the true stresses and true strains determined from torsion tests can be influenced by specimen geometry and the applied evaluation model. Numerical simulations of the torsion tests can be used to check the evaluated experimental results. The dependence of the flow stress on temperature and strain rate determined by hot compression tests up to a strain of about 0.6 was confirmed by the hot torsion tests.

A friction test setup which enables large plastic deformation of the sample under the nearly same loading case as in real extrusion was suggested. The developments of total force, friction force and temperatures were experimentally determined. It was found that friction stress depends strongly on temperature and sliding velocity. Different numerical models in HyperXtrude and ABAQUS/Explicit were used to simulate the friction tests. The best agreements between experiment and simulation were obtained with ABAQUS/Explicit using a combination of the Eulerian formulation for the sample and the Langrangian formulation for punch, die and mandrel. The Coulomb friction model in ABAQUS with a friction coefficient which depends on sliding velocity is suitable for the simulations of the friction tests.

Extrusion tests on circular rods and U-profiles performed at FZS Berlin were simulated with HyperXtrude and ABAQUS/Explicit The developments of microstructure like grain size and recrystallized volume fraction in extruded rods and profiles were investigated by means of metallographic investigation and EBSD analysis. A strong influence of process conditions (extrusion ratios, billet temperatures, product velocities and cooling conditions) on formation of microstructure was determined. An empirical model for modeling of recrystallization was applied to calculate the microstructure development in different extrusion products. The model parameters determined by fitting selected extrusion tests on rods were applied to other extrusion tests on rods and U-profiles. The computed microstructure is in good agreement with the experimental results.

ACKNOWLEDGMENTS

This work has been funded with budget funds of the Federal Ministry of Economic Affairs and Energy (BMWi) via the German Federation of Industrial Research Associations „Otto von Guericke“ e.V. (AiF) (IGF-Nr.: 18276 N) and supported by the Association of Metals (WVM). The authors would like to thank all parties involved for the funding and the support.

REFERENCES

Bai, Y., & Wierzbicki ,T. (2010). Application of extended Mohr–Coulomb criterion to ductile fracture. *Int. J. Fract.* 161:1–20.

Behrens, B.-A., Alasti, M., Bouguecha, A., Hadifi, T., Mielke, J., and Schäfer, F., Numerical and experimental investigations on the extension of friction and heat transfer models for an improved simulation of hot forging processes, *Proceedings of the 12th ESAFORM Conference on Material Forming*, Enschede (Netherlands), 27–29 April 2009.

DEFORM 3D Version 10.0 *User's Manual*, Scientific Forming Technologies Corporation, 2009

Dieter, G. E., Mechanical Metallurgy. *3rd ed., Mc Graw-Hill Book Co.*, New York 1986.

Hora, P., Gorji, M., and Berisha, B., Modeling of friction phenomena in extrusion processes by using a new torsion-friction test, Key Engineering Materials, Vol. 491, 2012, pp. 129-135, □(2012) *Trans Tech Publications*, Switzerland.

Karadogan, C., Grueebler, R., and Hora, P., A new cone-friction test for evaluating friction phenomena in extrusion processes, *Key Engineering Materials*, Vol. 424, 2010, pp. 161-166.

Mehtedi, M. El, Spigarelli, S., Gabrielli, F., Donati, L., Comparison study of constitutive models in predicting the hot deformation behavior of AA6060 and AA6063 Aluminium alloys, Aluminium Two Thousand World Congress and International Conference on Extrusion and Benchmark ICEB 2015, *Materials Today: Proceedings 2* (2015) 4732 – 4739.

Ockewitz, A., Sun, D.-Z., Andrieux, F., and Mueller, S., Key Engineering Materials, Vol. 491, 2012, pp. 257-264, □(2012) *Trans Tech Publications*, Switzerland.

Schikorra, M., Donati, L., Tomesani, L., Tekkaya, A.E., Microstructure analysis of aluminum extrusion: Prediction of microstructure on AA6060 alloy, *Journal of Materials Processing Technology*, vol. 201 (2008) pp. 156-162.

Sheppard, T., Duan, X., Modelling of static recrystallisation by the combination of empirical models with the finite element method, *Journal of Materials Science*, vol. 38 (2003) pp. 1747-1754.

Sun, D.-Z., Mueller, S., Verbesserte Simulation des Strangpressens von Aluminiumprofilen mit Gefügeberechnung, Schlussbericht, AiF-Förderkennzeichen: 18276 N, 2017.